Low Triphenyl phosphate concentrations fuel proliferation and migration of Hep3B, a hepatocellular carcinoma cell line

Shuqing Zhou (zhoushuqin@smu.edu.cn)
Southern Medical University
Liang Ye
Southern Medical University
Xu Zhang
the First Affiliated Hospital of Nanjing Medical University
Peng Wang
Southern Medical University
Ying Zhang
Southern Medical University
Shujiao He
Southern Medical University
Yang Li
Southern Medical University
Shao Li
Southern Medical University
Kangyan Liang
Southern Medical University
Shuguang Liao
Southern Medical University
Yi Gao
Southern Medical University
Qing Peng
Southern Medical University

Research Article

Keywords: Triphenyl phosphate,Proliferation,Migration,Hepatocellular carcinoma,Environmental toxicology

Posted Date: March 15th, 2022

DOI: https://doi.org/10.21203/rs.3.rs-1436756/v1

Abstract

Organophosphate flame retardants (OPFRs) have been widely used due to their unique properties. The OPFRs are mainly metabolized in the liver. However, whether the OPFRs in human plasma mediate progression of liver cancer remains unclear. Triphenyl phosphate (TPP) is one of the OPFRs that are most detected in environmental matrices. In this study, we performed CCK8, ATP, and EdU analyses to evaluate the effect of TPP (0.025–12.8μM concentration) on proliferation, invasion, and migration of Hep3B, a hepatocellular carcinoma cell line. Tumor-bearing mouses model were used for in vivo validation. The results showed that relative low concentrations (0.025 to 0.1μM) slightly increased cell proliferation and remarkably promoted cell invasion and migration of Hep3B. Animal experiments confirmed that TPP treatment significantly enhanced tumor growth in the xenograft HCC model. To explore the possible molecular mechanisms that might be mediating the actions of TPP on Hep3B, we profiled gene expression in groups treated with or without TPP (0.05 and 0.1μM) using transcriptional sequencing. Gene ontology (GO), Kyoto Encyclopedia of Genes and Genomes (KEGG) enrichment and Protein-Protein Interaction (PPI) analyses demonstrated that pathways affected by differentially expressed genes (DEGs) were mainly in nuclear-transcribed mRNA catabolic processes, cytosolic ribosome and ATPase activity. 0.05 and 0.1μM TPP led to up-regulation of a series of genes including EREG, DNPH1, SAMD9, DUSP5, PFN1, CKB, MICAL2, SCUBE3, and CXCL8, but suppressed the expression of MCC. These genes have been shown to be associated with proliferation and movement of cells. Together, our findings suggest that relatively low concentrations of TPP could fuel the proliferation, invasion, and migration of hepatocellular carcinoma cells. Thus, TPP might be a risk factor in the progression of hepatocellular carcinoma in humans.

Introduction

Flame retardants (FRs) are often used to prevent combustion and slow the spread of flames. Brominated flame retardant (BFR) accounted for a large proportion of the FRs [1]. However, due to regulatory requirements, environmental monitoring and growing concerns about persistence, accumulation, and toxicity of the BFRs, their use has gradually diminished [2]. Instead, organophosphate flame retardants (OPFRs), a class of artificial organic compounds, have been widely produced and adopted for use in plastics, indoor furniture, lubricants, decorative coatings, or textile [3], due to the presumption that they are less persistent and have minimal accumulation. The OPFRs include Tris (1,3-dichloro-isopropyl) phosphate (TDCIPP), triphenyl phosphate (TPP), tris (2-chloro-2-ethyl) and phosphoric acid (TCEP), etc [4]. By 2015, world-wide production of phosphate esters had increased to 680000 tons[5].

Most of the OPFRs have ester properties and physically bind to the final product rather than covalently attachment to the surface of the material [6]. They could be released from the product surfaces via abrasion and volatilization, as well as contact with the human body through ingestion, inhalation of dust particles and skin absorption[7]. Although the phosphate esters undergo rapid metabolism in organisms, data on their biological effects and related toxicity remains scant[8]. According to existing studies, Existing data has shown that the OPFRs have adverse effects in organisms. For instance, Tris (1,3-

dichloro-isopropyl) phosphate (TDCIPP) was shown to be a mutagen, as well as a potential neurotoxin and endocrine disruptor [9]. Subsequently, TDCIPP was included in the list of Chemicals in Proposition 65 (Cal, 2005), a potential carcinogen [1]. In addition, the OPFRs are endocrine disrupting chemical (EDCs) [10, 11]. Long-term exposure to OPFRs such as dioxin and dichloro diphenyl trichloroethane (DDT) might increase the risk of lung and breast cancers by disrupting the endocrine system. Triphenyl phosphate (TPP) can promote the proliferation and migration of prostate cancer cells and aggravate the progression of prostate cancer[12]. It has been reported that the concentration of OPFRs in blood samples of people with gastrointestinal cancers is nearly 100 times higher than that in normal people (0.3nM), suggesting that the OPFRs might also be risk factors for gastrointestinal cancers [13]. Liver is supposed to be the main accumulation and metabolism tissue for OPFRs [14, 15]. Primary liver cancer (PLC) is the only cancer with an increasing annual incidence among the top five deadliest cancers. It ranks fifth in the United States, and the incidence of liver cancer is higher in developing countries [16]. China accounts for 55 percent of the global PLC cases. The disease burden has remained high for 20 years, with no significant improvement in the 5-year survival rate [17]. Risk factors associated with liver cancer include hepatitis B, fatty liver, alcoholic cirrhosis, and dietary exposure [18]. Although environmental factors have also been associated with liver cancer, they have attracted less attention. There are currently very few studies that demonstrate the relationship between the exposure to OPFRs and development of liver cancer. Therefore, there is need for studies evaluating the potential risk of OPFRs in liver cancer.

About 11 OPFRs have been assessed in marine organisms. Out of the total, TPP was one of the most detected compounds, with a concentration ranging from 21 to 180ng/g [19]. Although TPP has been reported to be toxic to human hepatoma cell lines (hepG2, hepRG) and human normal liver cell line (LO-2), the concentrations that could induce toxicity were relatively high (> 10μM), which are less likely to be achieved in plasma and liver tissues [20, 21]. Data on the relationship between relatively low concentration TPP and progression of human liver cancer remains limited.

Here, we investigated the effects of TPP on hepatocellular carcinoma cells. We employed EdU and CCK8 cell proliferation assays to detected changes in cell proliferation ability, and then used transwell assay, wound healing assay and 3D Spheroid Invasion assay to analyze the differences in cell invasion and migration ability. In addition, we used transcriptome sequencing and qRT-PCR to compare and verify the gene expression differences in the liver cancer cells. The results showed that exposure of hepatoma cells to 30 ~ 60nM TPP plasma concentration [13] enhanced the proliferation and invasion ability of the cells.

Materials And Methods

Chemicals and reagents

TPP was purchased from Bidepharm (Shanghai, China), while Dulbecco's modified Eagle's medium (DMEM) and Penicillin-Streptomycin solution was purchased from BasoMedia (Shanghai, China). Fetal bovine serum (FBS) was obtained from Gibco (Beijing, China), while Cell Counting Kit-8 (CCK-8) was purchased from Dojindo Chemical technology (Shanghai co. LTD, Shanghai, China). In addition, EdU (5-

Ethynyl-2'-deoxyuridine) Cell Proliferation Kit with Alexa Fluor 488 and Enhanced ATP Detection kit was obtained from Beyotime (Guangzhou, China). All the experiments were carried out at least in triplicate.

Cell culture and treatment

Hep3B was obtained from iCell Bioscience Inc (Shanghai, ATCC), and were cultured in DMEM media, supplemented with 10% FBS and antibiotics (100 units/mL penicillin and 0.1mg/mL streptomycin). The cells were incubated at 37°C under a humidified 5% CO_2 atmosphere. The cells were passaged every 3 days and then used for experiments in exponential growth phase. Before exposure to TPP, the cells were seeded into 6-well plates, 12-well plates, or 96-well plates (Corning), and then cultured for 24 h. Then fresh culture medium with different concentrations of TPP was added and incubated for the same period (unless otherwise indicated). All the compounds were dissolved in DMSO with a final concentration of 0.1% (v/v). Controls were treated with the corresponding vehicle alone.

Cell Counting Kit-8 Assay

Cell viability was measured using the CCK-8 assay by counting the number of viable cells after various treatments. Briefly, five replicates of the Hep3B cells were seeded in 96-well plates at a cell density of 3,000 cells per well for 24 h. The cells were exposed to fold-ratio dilution concentrations of TPP for 48 or 72 h. After the TPP treatment, 10μL of CCK-8 reagent in 90μL DMEM per well was added to the cell culture medium, and then incubated at 37°C for 2 h. Absorbance was measured 6 times/well at 450 nm using an automatic microplate reader (Synergy4; BioTek, Winooski, VT, USA).

ATP detection assay

The metabolic activity and functional status of the cells were measured by the ATP expression assay using different processes. Firstly, the Hep3B cells were seeded in 6-well plates at a cell density of 200,000 cells per well for 24h. Thereafter, the cells were exposed to various concentrations of TPP (0, 0.025, 0.05, 0.1, 0.2, 0.4, 0.8, 1.6, 3.2, 6.4, 12.8μM) for 48h, followed by addition of 200μL lysate solution to each well. Pipettes were used to repeatedly blow or shake the culture plate to lyse the cells. The cell lysates were centrifuged at 12000g for 5min, and the supernatant was extracted for analysis. 100μL ATP detection liquid and 20μL of the supernatant samples were added to a 96-well blackboard (Corning) with five replicates for 3min. Luminescence (RLU) was measured by luminoskanTM Ascent Chemiluminescence instrument (Thermo Fisher technology Co. LTD, Shanghai, China).

EdU cell proliferation assay

Cell proliferation was measured by the EdU assay by counting the ratio of proliferated cells in total cells. Hep3B cells were seeded in 12-well plates at a cell density of 30,000 cells per well for 24h. The cells were

then exposed to various concentrations of TPP (0, 0.025μM, 0.05μM, 0.1μM and 0.2μM) for 48h. Afterwards, the plated cells were washed three times with PBS and then 1μL of EdU reagent (10mM) in 1mL DMEM with 10% FBS was added. The mixture was incubated at 37°C for 2 h and then fixed in 4% formaldehyde for 30 min at room temperature. After washing 3 times with 3% BSA solution, the cells were permeabilized in 0.3% Triton X-100 for 30 min at room temperature and then washed three times with 3% BSA, 5min per wash. The samples were mixed with click additive solutions, such as Click Reaction Buffer, CuSO4, Azide 488 and Click Additive Solution, then incubated at room temperature for 30min and in darkness. The nuclei were labeled with Hoechst33342. All immunofluorescence images were acquired using a Zeiss Axiovert A1 inverted fluorescence microscope and ImageJ 1.48k software was used for image processing. Changes in brightness or contrast during processing were applied equally across the entire images.

Transwell assay

To examine the invasive ability of the tumor cells, 8.0μm pore-size Transwell chambers were added into a 24-well plate, which was divided into the upper and lower chambers. Hep3B cells were seeded in 6-well plates at a cell density of 200,000 cells per well for 24h. The cells were then exposed to various concentrations of TPP (0, 0.025μM, 0.05μM, 0.1μM and 0.2μM) for 48h. Thereafter, 600μl of media with 10%FBS was added to the lower chamber, while 200 serum-free conditioned medium with 30,000 cells was added to the upper chamber. The cells were incubated at 37°C for 36 h, and then the upper chamber cells were wiped with cotton swabs. Invasion cells were fixed and stained with crystal violet for counting.

Wound healing assay

Before exposure to TPP, Hep3B cells were seeded in 6-well plate and cultured in DMEM media containing 10% FBS for 24h. At a cell confluence of 100%, wounds were scratched on the cell monolayer using a 200μL pipette tip. The plates were washed twice with PBS, and then the cells were incubated in DMEM with 1% FBS containing various concentrations of TPP (0, 0.025μM, 0.05μM, 0.1μM and 0.2μM) for 72-96h. The wounded areas were imaged with ICX41 inverted bright field microscope at the same period. The area difference was calculated using ImageJ software (NIH, USA). Three different areas were selected and used to estimate the distance of the migrating cells in each assay, and the assay was carried out as previously described.

3D Spheroid Invasion Assay

This scheme provides an overview for the measurement of 3D Tumor Single Spheroid cell invasion into surrounding extracellular matrix (corning) to compare the invasion ability of cells under different treatment conditions. Hep3B cells were seeded into 96-well round bottom, ultra-low attachment plate (Corning® Cat. No. 7007) at a density of 3,000 cells per well and centrifuged at 125g for 10 min. The cells

were then cultured in 200μL DMEM containing 10% FBS and incubated at 37°C for 24-48h. At the formation of spheroids, the supernatant was removed and placed on a pre-chilled Coolsink 96F within a Coolbox 96F box for about 5-10 minutes. Matrigel stock was diluted to 2x final assay concentration (prepared 8mg/ml Matrigel for a final assay concentration of 4mg/ml) in DMEM medium with 10%FBS in a cold polypropylene tube. Using pre-chilled pipette tips and reverse pipetting technique, 90 μL of the diluted Matrigel was slowly added into appropriate wells. This method utilized IncuCyte® Live-Cell Analysis System (Essen BioScience, A Sartorius Company) for kinetic, image-based bright field and fluorescence measurements of spheroid invasion (invading cells and whole spheroid areas). After incubation at 37°C for 30min, and at matrix polymerization, 100μl/well of DMEM complete culture media containing various concentrations of TPP (0, 0.025μM, 0.05μM, 0.1μM and 0.2μM) or media alone was added into the plates and then returned to the IncuCyte® to monitor spheroid invasion (every day for 12 days). The dimension of the spheroids was calculated using ImageJ software (NIH, USA).

Animal studies

Male Balb/c nude mice (4–5-weeks-old) were purchased from the Animal Experimental Center of Southern Medical University. The animal study was carried out in strict accordance with the Guidelines for the Care and Use of Laboratory Animals, China. All experimental protocols involving animals were approved by the Laboratory Animal Ethics Committee of Zhujiang Hospital of Southern Medical University (approval document number:LAEC-2021-196), The Hep3B cells at density of 1×10^7 in 1ml of PBS were inoculated subcutaneously into the left flank of the nude mice. When the mice were housed for one weeks, the mice were randomly assigned to the vehicle control(n=3) and treated groups(n=3), and they were treated with 5% glucose solution (control) and 1mg/kg TPP solution by intraperitoneal administration, three times in one week, with one or two days intervals, respectively. After treatment for 14 days, the mice were sacrificed after the final therapy. Tumors were removed and their mean diameter was measured.

RNA isolation and quantitative real-time RT-PCR

The genes related to cell migration and invasion were validated using real-time PCR (RT-PCR). Briefly, RNA was extracted by TRIzol regent (ThermoFisher technology (China) co. LTD, Shanghai, China), following the manufacturer's instruction. We then used Nanodrop 2000 (Thermo Fisher Scientific) to quantify the extracted RNA ensuring the ratio of 260/280 between 1.8 and 2.0, and then cDNA was synthesized using reverse-transcription. Next, the cDNA was quantified by real-time PCR with SybrGreen qPCR master Mix (Thermo Fisher technology co. LTD, Shanghai, China). Results were normalized to the expression of GAPDH. The $2^{-\triangle\triangle Ct}$ method was used to calculate the expression levels.

RNA sequencing

Next generation mRNA-Sequencing (mRNA-seq) was performed for Hep3B cells. Briefly, after one week of treatment with 0.05uM and 0.1uM TPP, the cells were collected and underwent RNA extraction. The sequencing library was prepared and then sequenced in Illumina HiSeq X10 instrument (Guangzhou Ruijie Biological Co. Ltd). We used FPKM to evaluate the mRNA expression level. In addition, DESeq R package was used to conduct differential expression analysis. Corrected p-value was set at 0.05 and the absolute value of log 2 FC (fold change) was set at ≥ 1 as the threshold for differentially expressed genes (DEGs).

Enrichment analysis of TPP-related genes

After screening for the differentially expressed genes, we conduct further analysis based on the biological and molecular functions of the DEGs. Four packages, “clusterProfiler”, enrichplot”, “org.Hs.eg.db” and “ggplot2”, in R were used to perform Gene Ontology (GO) and Kyoto Encyclopedia of Genes and Genomes (KEGG) pathway enrichment analysis. In GO enrichment analysis, we analysed the Biological process (BP), molecular function (MF) and cellular component (CC). A $P < 0.05$ was used as the threshold in the analysis.

Protein-protein interaction (PPI) network

To explore the roles, if any, of the proteins encoded by the DEGs, STRING (https://www.string-db.org/) was used to construct a PPI network. Thereafter, Cytoscape 3.8.2 was used to analyze and visualize the PPI network. Genes with over 20 degrees were considered pivot genes.

Statistical analysis

The results were presented in form of average±standard deviation, and all the statistical analysis was performed in GraphPad Prism 9.0. One-way or Two-way ANOVA was used to evaluate the differences among the study groups. Statistical analysis between two groups was performed using the two-tailed unpaired Students’ T-test. The symbols used for statistical significance were ****($p<0.0001$), ***($p<0.001$), **($p<0.01$) and *($p<0.05$). Six replicates were performed for the statistical analysis, and the data obtained were from three independent and repeated groups.

Results

Exposure to low concentration of TPP enhanced the proliferation of Hep3B cells.

To study the biological effects of TPP on Hep3B cells and minimize cytotoxicity, appropriate concentration was selected according to the cell viability test. The results of CCK8 demonstrated that the

TPP IC50 was about 270μM, and there was no obvious cell cytotoxicity when exposed to low concentrations of TPP (0.025 ~ 3.2μM) from 24h to 72h (Figure 1a). The results indicated that TPP had toxic effect on the hepatocellular carcinoma cell line when exposed to 6.4μM for 24h or more. These results were in sync with a previous report [4]. However, exposure of the cells to 0.2 μM or less of TPP for 48 h or more led to a proliferative effect by nearly 25%, an observation that was further verified by the EdU cell proliferation test (Figure 1c and d). The results showed that the proportion of proliferating cells in the control group or in the group treated with low concentration of TPP was 15-20% or 35-55%, respectively in a 2 h culture period. In order to explore the specific situation of intracellular energy metabolism, intracellular ATP content was detected. The data demonstrate higher ATP synthesis in the low concentration group (0.025-0.1μ M)(Figure 1b).

TPP exposure enhanced the migration and invasion of the Hep3B cells

To reduce the cytotoxicity and eliminate the inhibitory effect of high concentration of TPP compound on cell activity. Based on the cell viability test, a relatively low concentration range (0.025, 0.05, 0.1,0.2 μ M) was used to determine the biological effects of TPP on cells. The wound healing assay(Figure 2c), 3D Spheroid Invasion assay (Figure 3a)and Transwell assay(Figure 2a) showed that TPP could promote the migration of the Hep3B cells in a concentration-dependent manner. Besides, the number of invasive cells increased significantly .

According to the results of Transwell experiment, the invasiveness of Hep3B cells exposed to TPP at low concentrations (0.025μM and 0.05μM) was significantly enhanced. With the increase of TPP exposure concentrations (0.1μM and 0.2μM), the invasiveness of liver cancer cells gradually decreased. The 3D Spheroid Invasion assay showed that compared with the control group, Hep3B cells exposed to low concentrations of TPP (0.025μM, 0.05μM and 0.1μM) had a relatively enhanced ability of Spheroid Invasion. For the TPP exposed group with a relatively high concentration (0.2μM), the difference in spheroid invasion disappeared. According to cell scratch results, the migration ability of liver cancer cells exposed to low concentration gradient of TPP increased to a certain extent. Concentration dependence is not obvious.

TPP enhanced the growth of HCC xenografts in vivo

We next established a xenograft HCC model to evaluate the biological effect of TPP in vivo. Hep3B xenograft-bearing mice were treated with 1mg/kg TPP three times a week. After the final treatment on day 14, all the nude mice were sacrificed, and tumors were resected, imaged and measured. The result of animal experiments showed that TPP treatment significantly enhanced tumor growth in the xenograft HCC model compared to the vehicle groups (Figure 3c). Taken together, these findings suggest that TPP has a potential risk on HCC xenografts.

Analysis of the differentially expressed genes related to TPP and Hepatocellular Carcinoma

RNA-seq data from next generation mRNA-sequencing was used to analyze DEGs between the TPP-treated and control group (untreated group). The results demonstrated that there were a total of 1021 down-regulated and 540 up-regulated genes in the Hep3B cells under treatment with 0.05μM TPP, compared with the control Hep3B cells(Figure 4). In addition, there were a total of 287 down-regulated and 115 up-regulated genes in the Hep3B cells treated with 0.1μM TPP (Figure 5).

Function and interaction analysis of the differentially expressed genes

To explore the potential functions enriched in the TPP and hepatocellular carcinoma, we performed GO and KEGG enrichment analysis (Figure 5). GO enrichment analysis showed that the BPs were mostly related to nuclear-transcribed mRNA catabolic processes, SRP-dependent co-translational protein targeting to membrane, nonsense-mediated decay. In terms of CC, the most enriched terms included cytosolic ribosome, ribosomal subunit, ribosome, polysomal ribosome, cytosolic large ribosomal subunit, and cytosolic small ribosomal subunit. In addition, structural constituents of the ribosome, ATPase activity, signaling adaptor activity, lysine-acetylated histone binding and acetylation-dependent protein binding were also significantly enriched in MF(Figure 5).

PPI network

To determine the roles of the DEGs in TPP and hepatocellular carcinoma, we employed Cytoscape to analyze the PPI network. The PPI network had a total of 172 nodes and 765 edges (Figure 4). The venn diagram also showed that MCC, SCUBE3, EREG, DNPH1, SAMD9, DUSP5, PFN1, CKB, MICAL2 and CXCL8 might be playing an important role in TPP-induced hepatocellular carcinoma. These hub genes showed a certain correlation with other genes in the network, revealing that they might be affecting hepatocellular carcinoma progression.

Identification of DEGs using real-time fluorescence quantitative RT-PCR

Like the RNA-seq data, we screened for DEGs in TPP treated and control group using qRT-PCR, and highlighted genes related to cell proliferation phenotype (EREG, DNPH1, SAMD9, MCC and DUSP5) and cell invasion phenotype (PFN1, CKB, MICAL2, SCUBE3 and CXCL8). The expression differences of some mRNA were more significant than the results of sequencing (Figure 6). Besides, the common indexes related to expansion and invasion of hepatocellular carcinoma cells such as EGF, EGFR, E-cadherin, N-

cadherin, PCNA and Ki-67 were detected by PCR. EGF, EGFR and N-cadherin genes were slightly up-regulated while E-cadherin was slightly down-regulated in the TPP-treated group. There was no statistically significant difference in the expression of PCNA and Ki-67 among different groups (Figure 6).

Discussion

With the increased use of phosphate flame retardants, more attention has been paid to the biological effects of phosphate esters. Although OPFR has less biological accumulation or environmental toxicity compared with BFR, most of the OPFRs and its metabolites have been shown to be toxic to the lung, liver, and reproductive system [22]. A few studies have shown that these compounds have certain carcinogenic effects [23]. Besides, some epidemiological studies have indicated that a considerable degree of TPP concentration can be detected in human urine. The enrichment level of serum TPP in different cancer populations in some areas was nearly 100-fold higher than that in normal population [13, 24]. It is thought that there could be a positive correlation between serum TPP level, and gastrointestinal cancer and colorectal cancer.[13]The study confirmed that TPP aggravates the malignancy and progression of prostate cancer cells by inducing cancer cell migration, proliferation as well as increasing the heterogeneity of the cells. However, there is little information available on the potential association between TPP exposure and liver cancer. In this study, we investigated the effects of TPP on hepatocellular carcinoma cells by detecting its influence on proliferation, migration, and invasion of Hep3B cells. The CCK8, ATP and EdU proliferation assay results showed that the biological effects of TPP on Hep3B cells were dependent on concentration range(Fig. 1). Consistent with previous reports [4, 25, 26], exposure of the Hep3B cells to TPP concentrations of above 6.4μM, led to lower cell activity, significantly suppressed cell proliferation, as well as ATP production(Fig. 1). When the cells were exposed to moderate concentration of TPP (0.2–3.2 μM), there was no significant change in cell phenotypic characteristics. However, enhancement on cell proliferation activity and cell invasion could be detected when the Hep3B cells were exposed to relatively low concentration of TPP (0-0.2 μ M), and the most robust change was demonstrated at a concentration of 0.05μM. We hypothesized that this range of TPP concentrations was achievable in human plasma, as it was reported that the concentration of OPFRs in blood samples of gastrointestinal cancers patients ranged from 0.03 to 0.06 μM.

We next assessed the changes in cell migration and invasion. To detect the effect of TPP on cell migration and invasion, we performed Transwell and wound healing assays(Fig. 2). The results demonstrated that treatment with low concentrations of TPP (0.025 -0.1μ M) could dramatically enhance the invasion ability of the Hep3B cells. We then conducted the 3D spheroid invasion assay to verify the above results(Fig. 3). We selected the 3D tumor spheroids as a cell model for invasion detection was because, unlike traditional models, this model could enable the tumor cells to be organized into a 3D structure thus mimic a tumor micro-region or a micro-metastasis, the tumor spheroids are highly reproducible in size, and enables both high content and high throughput analyses of tumor cell invasion [27]. The results of the spheroids invasion experiment showed no significant difference in the initial stage of spheroid formation. After a week of culturing, there was an outward invasion and growth of cell spheroids to the matrix gel which was apparently induced by low concentrations of TPP treatment. Next,

we carried out animal experiments to further confirm the effect of TPP in vivo. The results of animal experiments showed that TPP can significantly promote the growth of hepatocellular carcinoma in vivo(Fig. 3). This evidence suggests that TPP may have some potential carcinogenic effects. Taken together, these data demonstrated that the level of human blood TPP might affect the progression of liver cancer and even lead to the occurrence of hepatocellular carcinoma.

To further explore the molecular mechanisms that might be mediating the effects of the low concentrations of TPP on the hepatocellular carcinoma cell phenotypes, we analyzed gene expression shifts in groups the control and TPP-treated group (0.05 μM and 0.10 μM) using transcriptional sequencing. The results showed that 1561mRNAs were up and downregulated in the low concentration treatment group. Out of the total mRNAs, 541 were up-regulated while 1020 were downregulated. Only 402 mRNA expression differences were found in middle-low concentration treatment group(Fig. 4). GO and KEGG enrichment analysis indicated that a large proportion of the DEGs were enriched in pathways associated with ATPase and motor activity, and most of these genes were up regulated(Fig. 5). These data further suggested that low TPP concentrations might be enhancing the proliferation and invasion of hepatocellular carcinoma cells by interfering with cellular metabolism and motility related pathways.

In addition, to evaluate the genes related with TPP specific cellular phenotypic changes in the Hep3B cells, the respective DEGs and crosstalk DEGs in the 0.05μm and 0.1μm TPP-treated groups were analyzed. The functions of the DEGs were identified using Genecards and NCBI Gene database. The data showed that the expression of several DEGs related to proliferation and migration phenotypes were strikingly similar between the two treatment groups(Fig. 4). The DEGs related to cell proliferation included EREG, DNPH1, SAMD9, MCC and DUSP5. These genes (except MCC) were positively correlated with cell proliferation and were up-regulated in different treatment groups. EREG encodes a member of a secretory peptide hormone and epidermal growth factor (EGF) protein family. The encoded protein is a ligand of epidermal growth factor receptor (EGFR) and structure-related erb-b2 receptor tyrosine kinase 4 (ERBB4). Previous studies have shown that EREG participates in inflammation, wound healing, and cell proliferation (REF). In addition, EREG coding proteins might promote the progression of cancer in a variety of human tissues [28]. Real time PCR results (Fig. 6) confirmed the findings that both EGF and its binding site EGFR were up-regulated. On the other hand, SAMD9 protein is localized in the cytoplasm and plays an important role in regulating cell proliferation and apoptosis [29]. The protein encoded by DUSP5 is a member of the double specific protein phosphatase subfamily. The family negatively regulates the members of the mitogen activated protein (MAP) kinase superfamily (MAPK/ERK, SAPK/JNK, p38), which are related to cell proliferation and differentiation, and are prognostic indicators of thyroid follicular carcinoma [30]. DNPH1 gene was identified based on c-Myc protein stimulation (REF). The latter is a transcription factor involved in regulating cell proliferation, differentiation and apoptosis. However, the exact functions of the gene is not well defined. Recent data has shown that targeting DNPH1 makes BRCA-deficient cells sensitive to PARP inhibitors in the treatment of breast and ovarian cancer [31]. PCR results showed that MYC expression was also activated in TPP treated groups. Cell migration related differential genes included PFN1, CKB, MICAL2, SCUBE3 and CXCL8. These genes were positively correlated with the ability of cell migration and invasion, and the trend in changes was the same in both

TPP treatment groups. PFN1 encodes a member of the profilin family of small actin binding proteins. The protein regulates actin polymerization and plays an important role in actin kinetics. A previous study showed that a PFN1 transcript is negatively regulated by miR-19a-3p and inhibits malignant progression of human hepatocellular carcinoma [32]. The MICAL2 is a monooxygenase, which can enhance depolymerization of F-actin, participates in cytoskeleton dynamics and acts as a regulator of SRF signaling pathway. The increased expression of this gene mediates the progression and metastasis of cancer [33]. The protein encoded by CXCL8 is a member of the CXC chemokine family and acts as the main mediator of inflammatory response. This protein is also secreted by tumor cells and promotes tumor migration, invasion, angiogenesis and metastasis [34, 35]. The data of RNA-seq provided us many clues in the possible molecular mechanisms mediating the TPP-induced proliferation and migration of cells. However, further studies on the mechanisms involved in cell proliferation effects are still needed.

This study was limited by the fact that it only studied one hepatocellular carcinoma cell line. Thus, more liver cancer cell lines and primary hepatocellular carcinoma cell should be investigated subsequent studies.

Conclusion

Taken together, our study demonstrated that exposure to low TPP concentrations (close to the human blood concentration) might lead to enhanced proliferation and invasion ability of hepatocellular carcinoma cells. Therefore, TPP should be considered as a risk factor that could fuel the progression of hepatocellular carcinoma in humans.

Declarations

Availability of data and material

Data and materials used and/or analyzed during the current study are available from the corresponding authors on reasonable request.

Author contributions

LY was responsible for the main design and implementation of the experiment, and wrote the main manuscript text. XZ was responsible for data processing and bioinformatics analysis. PW and YZ were responsible for the repeated operation of the experiment. SH, YL and SL prepared the experimental figures for the whole article. SL, YG and KL were responsible for the preparation of experimental supplies. QP and SZ provided experimental guidance and manuscript revision.

Funding

The authors are grateful for the financial support by the National Key R&D Program of China (2018YFA0108200, 2018YFC1106400), the National Natural Science Foundation of China (22075127, 31972926), the Natural Science Foundation of Guangdong Province (2018A030313128, 2018A030313214), and the Guangdong Key Research and Development Plan (2019B020234003).

Conflict of interest

The authors declare that they have no conflict of interest.

Ethics approval

The animal study was carried out in strict accordance with the Guidelines for the Care and Use of Laboratory Animals, China. All experimental protocols involving animals were approved by the Laboratory Animal Ethics Committee of Zhujiang Hospital of Southern Medical University (approval document number:LAEC-2021-196)

Consent to participate

Informed consent was obtained where applicable.

Consent for publication

All authors have read and agreed to the published version of the manuscript.

References

1. Chen, R., Hou, R., Hong, X., Yan, S., & Zha, J. 2019. Organophosphate flame retardants (OPFRs) induce genotoxicity in vivo: A survey on apoptosis, DNA methylation, DNA oxidative damage, liver metabolites, and transcriptomics. Environment international, 130, 104914.
2. Percy, Z., Vuong, A. M., Ospina, M., Calafat, A. M., La Guardia, M. J., Xu, Y., Hale, R. C., Dietrich, K. N., Xie, C., Lanphear, B. P., Braun, J. M., Cecil, K. M., Yolton, K., & Chen, A. 2020. Organophosphate esters in a cohort of pregnant women: Variability and predictors of exposure. Environmental research, 184, 109255.
3. Tsugoshi, Y., Watanabe, Y., Tanikawa, Y., Inoue, C., Sugihara, K., Kojima, H., & Kitamura, S. 2020. Inhibitory effects of organophosphate esters on carboxylesterase activity of rat liver microsomes. Chemico-biological interactions, 327, 109148.
4. Wang, X., Li, F., Liu, J., Ji, C., & Wu, H. 2020. Transcriptomic, proteomic and metabolomic profiling unravel the mechanisms of hepatotoxicity pathway induced by triphenyl phosphate

(TPP). Ecotoxicology and environmental safety, 205, 111126.

5. Mennillo, E., Cappelli, F., & Arukwe, A. 2019. Biotransformation and oxidative stress responses in rat hepatic cell-line (H4IIE) exposed to organophosphate esters (OPEs). Toxicology and applied pharmacology, 371, 84–94.
6. Gbadamosi, M. R., Abdallah, M. A., & Harrad, S. 2021. A critical review of human exposure to organophosphate esters with a focus on dietary intake. The Science of the total environment, 771, 144752.
7. Xu, F., Giovanoulis, G., van Waes, S., Padilla-Sanchez, J. A., Papadopoulou, E., Magnér, J., Haug, L. S., Neels, H., & Covaci, A. 2016. Comprehensive Study of Human External Exposure to Organophosphate Flame Retardants via Air, Dust, and Hand Wipes: The Importance of Sampling and Assessment Strategy. Environmental science & technology, 50(14), 7752–7760.
8. Negi, C. K., Bajard, L., Kohoutek, J., & Blaha, L. 2021. An adverse outcome pathway based in vitro characterization of novel flame retardants-induced hepatic steatosis. Environmental pollution (Barking, Essex : 1987), 289, 117855.
9. Ding, J., Xu, Z., Huang, W., Feng, L., & Yang, F. 2016. Organophosphate ester flame retardants and plasticizers in human placenta in Eastern China. The Science of the total environment, 554-555, 211–217.
10. Cano-Sancho, G., Smith, A., & La Merrill, M. A. 2017. Triphenyl phosphate enhances adipogenic differentiation, glucose uptake and lipolysis via endocrine and noradrenergic mechanisms. Toxicology in vitro : an international journal published in association with BIBRA, 40, 280–288.
11. Liu, X., Ji, K., Jo, A., Moon, H. B., & Choi, K. 2013. Effects of TDCPP or TPP on gene transcriptions and hormones of HPG axis, and their consequences on reproduction in adult zebrafish (Danio rerio). Aquatic toxicology (Amsterdam, Netherlands), 134-135, 104–111.
12. Zhang, X., Lu, Z., Ren, X., Chen, X., Zhou, X., Zhou, X., Zhang, T., Liu, Y., Wang, S., & Qin, C. 2021. Genetic comprehension of organophosphate flame retardants, an emerging threat to prostate cancer. Ecotoxicology and environmental safety, 223, 112589.
13. Li, Y., Fu, Y., Hu, K., Zhang, Y., Chen, J., Zhang, S., Zhang, B., & Liu, Y. 2020. Positive correlation between human exposure to organophosphate esters and gastrointestinal cancer in patients from Wuhan, China. Ecotoxicology and environmental safety, 196, 110548.
14. Phillips, A. L., & Stapleton, H. M. 2019. Inhibition of Human Liver Carboxylesterase (hCE1) by Organophosphate Ester Flame Retardants and Plasticizers: Implications for Pharmacotherapy. Toxicological sciences : an official journal of the Society of Toxicology, 171(2), 396–405.
15. Van den Eede, N., de Meester, I., Maho, W., Neels, H., & Covaci, A. 2016. Biotransformation of three phosphate flame retardants and plasticizers in primary human hepatocytes: untargeted metabolite screening and quantitative assessment. Journal of applied toxicology : JAT, 36(11), 1401–1408.
16. Anwanwan, D., Singh, S. K., Singh, S., Saikam, V., & Singh, R. 2020. Challenges in liver cancer and possible treatment approaches. Biochimica et biophysica acta. Reviews on cancer, 1873(1), 188314.

17. Professional Committee for Prevention and Control of Hepatobiliary and Pancreatic Diseases of Chinese Preventive Medicine Association, Committee of Hepatology of Chinese Research Hospital Association, Society of Hepatology of Chinese Medical Association, & Prevention of Infection Related Cancer (PIRCA) Group, Specialist Committee of Cancer Prevention and Control of Chinese Preventive Medicine Association 2021. Zhonghua zhong liu za zhi [Chinese journal of oncology], 43(1), 60–77.
18. Marengo, A., Rosso, C., & Bugianesi, E. 2016. Liver Cancer: Connections with Obesity, Fatty Liver, and Cirrhosis. Annual review of medicine, 67, 103–117
19. Liu, C., Wang, Q., Liang, K., Liu, J., Zhou, B., Zhang, X., Liu, H., Giesy, J. P., & Yu, H. 2013. Effects of tris(1,3-dichloro-2-propyl) phosphate and triphenyl phosphate on receptor-associated mRNA expression in zebrafish embryos/larvae. Aquatic toxicology (Amsterdam, Netherlands), 128-129, 147–157.
20. An, J., Hu, J., Shang, Y., Zhong, Y., Zhang, X., & Yu, Z. 2016. The cytotoxicity of organophosphate flame retardants on HepG2, A549 and Caco-2 cells. Journal of environmental science and health. Part A, Toxic/hazardous substances & environmental engineering, 51(11), 980–988.
21. Van den Eede, N., Cuykx, M., Rodrigues, R. M., Laukens, K., Neels, H., Covaci, A., & Vanhaecke, T. 2015. Metabolomics analysis of the toxicity pathways of triphenyl phosphate in HepaRG cells and comparison to oxidative stress mechanisms caused by acetaminophen. Toxicology in vitro : an international journal published in association with BIBRA, 29(8), 2045–2054.
22. Ma, Y., Stubbings, W. A., Cline-Cole, R., & Harrad, S. 2021. Human exposure to halogenated and organophosphate flame retardants through informal e-waste handling activities - A critical review. Environmental pollution (Barking, Essex : 1987), 268(Pt A), 115727.
23. Liu, Y., Li, Y., Dong, S., Han, L., Guo, R., Fu, Y., Zhang, S., & Chen, J. 2021. The risk and impact of organophosphate esters on the development of female-specific cancers: Comparative analysis of patients with benign and malignant tumors. Journal of hazardous materials, 404(Pt B), 124020.
24. Feng, L., Ouyang, F., Liu, L., Wang, X., Wang, X., Li, Y. J., Murtha, A., Shen, H., Zhang, J., & Zhang, J. J. 2016. Levels of Urinary Metabolites of Organophosphate Flame Retardants, TDCIPP, and TPHP, in Pregnant Women in Shanghai. Journal of environmental and public health, 2016, 9416054.
25. Su, G., Crump, D., Letcher, R. J., & Kennedy, S. W. 2014. Rapid in vitro metabolism of the flame retardant triphenyl phosphate and effects on cytotoxicity and mRNA expression in chicken embryonic hepatocytes. Environmental science & technology, 48(22), 13511–13519.
26. Wade, M. G., Kawata, A., Rigden, M., Caldwell, D., & Holloway, A. C. 2019. Toxicity of Flame Retardant Isopropylated Triphenyl Phosphate: Liver, Adrenal, and Metabolic Effects. International journal of toxicology, 38(4), 279–290.
27. Clevers H. 2016. Modeling Development and Disease with Organoids. Cell, 165(7), 1586–1597.
28. Zong, S., Liu, X., Zhou, N., & Yue, Y. 2019. E2F7, EREG, miR-451a and miR-106b-5p are associated with the cervical cancer development. Archives of gynecology and obstetrics, 299(4), 1089–1098.
29. Nagamachi, A., Kanai, A., Nakamura, M., Okuda, H., Yokoyama, A., Shinriki, S., Matsui, H., & Inaba, T. 2021. Multiorgan failure with abnormal receptor metabolism in mice mimicking Samd9/9L

syndromes. The Journal of clinical investigation, 131(4), e140147.

30. Zhang, Q., Xing, Y., Jiang, S., Xu, C., Zhou, X., Zhang, R., Xie, T., Zou, Z., Gong, P., Zhu, H., Zhang, D., Ma, H., Liao, L., & Dong, J. 2020. Integrated analysis identifies DUSP5 as a novel prognostic indicator for thyroid follicular carcinoma. Thoracic cancer, 11(2), 336–345.
31. Fugger, K., Bajrami, I., Silva Dos Santos, M., Young, S. J., Kunzelmann, S., Kelly, G., Hewitt, G., Patel, H., Goldstone, R., Carell, T., Boulton, S. J., MacRae, J., Taylor, I. A., & West, S. C. 2021. Targeting the nucleotide salvage factor DNPH1 sensitizes BRCA-deficient cells to PARP inhibitors. Science (New York, N.Y.), 372(6538), 156–165.
32. Wang, Z., Shi, Z., Zhang, L., Zhang, H., & Zhang, Y. 2019. Profilin 1, negatively regulated by microRNA-19a-3p, serves as a tumor suppressor in human hepatocellular carcinoma. Pathology, research and practice, 215(3), 499–505.
33. Cai, Y., Lu, J., & Tang, F. 2018. Overexpression of MICAL2, a novel tumor-promoting factor, accelerates tumor progression through regulating cell proliferation and EMT. Journal of Cancer, 9(3), 521–527.
34. Liu, Q., Li, A., Tian, Y., Wu, J. D., Liu, Y., Li, T., Chen, Y., Han, X., & Wu, K. 2016. The CXCL8-CXCR1/2 pathways in cancer. Cytokine & growth factor reviews, 31, 61–71.
35. Lin, C., He, H., Liu, H., Li, R., Chen, Y., Qi, Y., Jiang, Q., Chen, L., Zhang, P., Zhang, H., Li, H., Zhang, W., Sun, Y., & Xu, J. 2019. Tumour-associated macrophages-derived CXCL8 determines immune evasion through autonomous PD-L1 expression in gastric cancer. Gut, 68(10), 1764–1773.

Figures

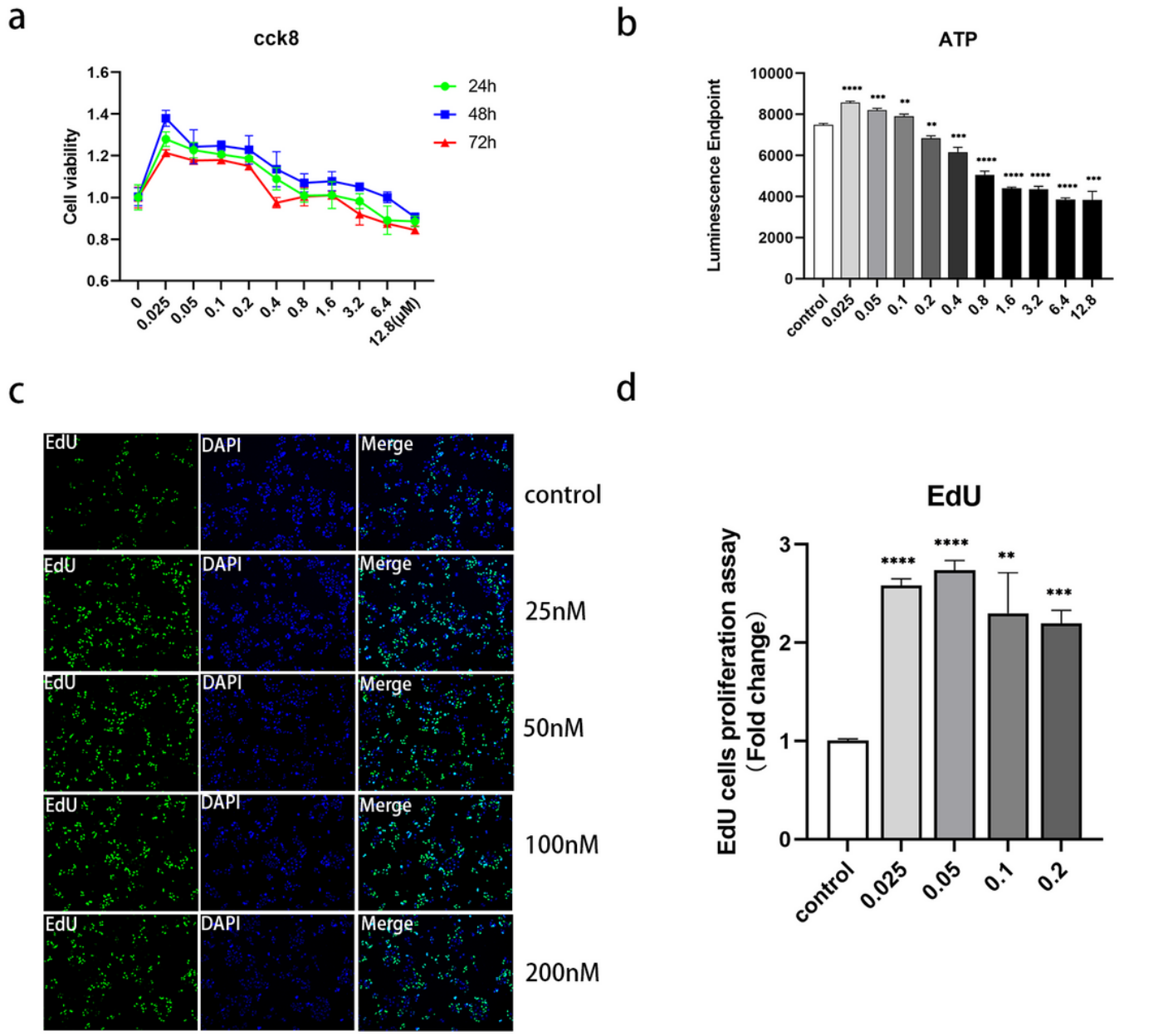

Figure 1

Possible effect of TPP exposure on Hep3B cell proliferation. (a) The viability of cells after exposure to different concentrations of TPP (0, 0.025, 0.05, 0.1, 0.2, 0.4, 0.8, 1.6, 3.2, 6.4, and 12.8μM) for 24h, 48h and 72h as determined by the CCK-8 assay. The TPP was dissolved in 0.1% DMSO as the vehicle. (b) ATP detection assay was carried out to determine the metabolic activity of cells after exposure to different concentrations of TPP (0, 0.025, 0.05, 0.1, 0.2, 0.4, 0.8, 1.6, 3.2, 6.4, and 12.8μM) for 48h. (c)The proliferation of cells was tested using the EdU assay. Cells were treated with different concentrations of TPP (0.025μM, 0.05μM, 0.1μM and 0.2μM) and cells in the control group were treated with 0.1% DMSO. (d) A graph showing results of EdU assay. The fold changes of the proportion of proliferating cells and mean-value of 0.025μM, 0.05μM, 0.1μM and 0.2μM were 2.55±0.07, 2.74±0.09, 2.35±0.42, and 2.16±0.14

compared to the control group (1±0.02). The error bars represent the mean±SD of at least three independent experiments. (n=3, ****(p<0.0001), ***(p<0.001), **(p<0.01) and *(p<0.05)).

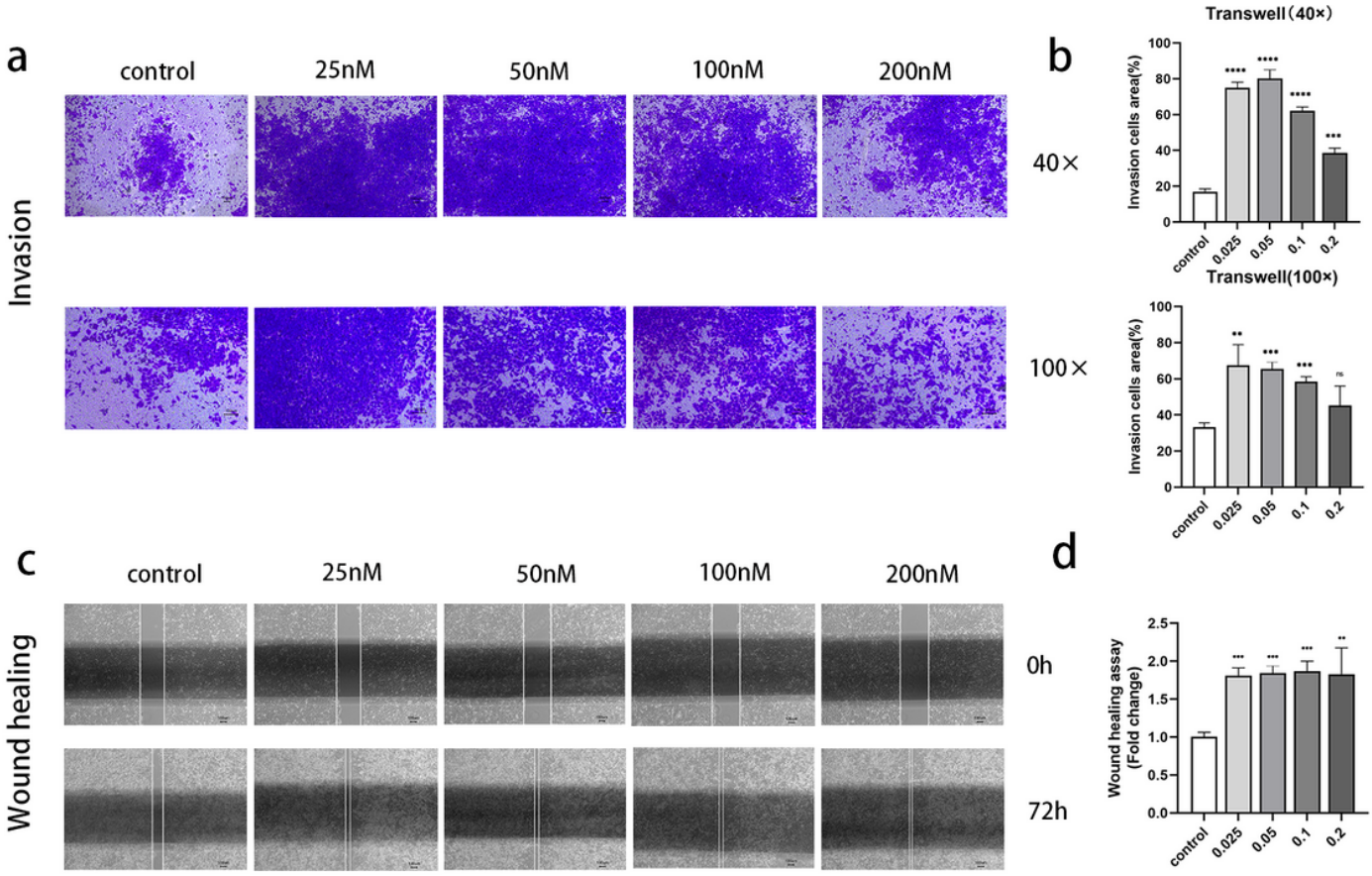

Figure 2

Potential effect of TPP exposure on Hep3B cell migration. (a) Cells were exposed to different concentrations of TPP (0.025μM, 0.05μM, 0.1μM and 0.2μM) and cells in the control group were treated with 0.1% DMSO. (a) Invaded Hep3B cells (40× and 100×). After exposure of TPP for 36h, invaded cells were stained with crystal violet. (b) A data graph showing results of the invasion assay. The invaded area

% (40×) of 0.025μM, 0.05μM, 0.1μM and 0.2μM was 75.03±3.08, 80.18±4.88, 62.21±2.11, and 38.62±2.63, respectively, compared to the control group (16.99±1.50). The invasion area% (100×) of 0.025μM, 0.05μM, 0.1μM and 0.2μM was 67.43±11.42, 65.42±3.65, 58.49±2.54, and 45.32±10.61, respectively, compared to the control group (33.19±2.21). (c) Migrated Hep3B cells (40×). The difference in the distance between scratched area at 0h and 72h represents the migration rate of cells. (d) A data graph showing results of the wound healing assay. The fold change of the distance between scratched area and mean-value of 0.025μM, 0.05μM, 0.1μM and 0.2μM was 1.81±0.10, 1.84±0.09, 1.87±0.13, and 1.82±0.42, respectively, compared to the control group (1±0.06). The error bar represents the mean±SD of at least three independent experiments. (n=3, ****(p<0.0001), ***(p<0.001), **(p<0.01) and *(p<0.05))

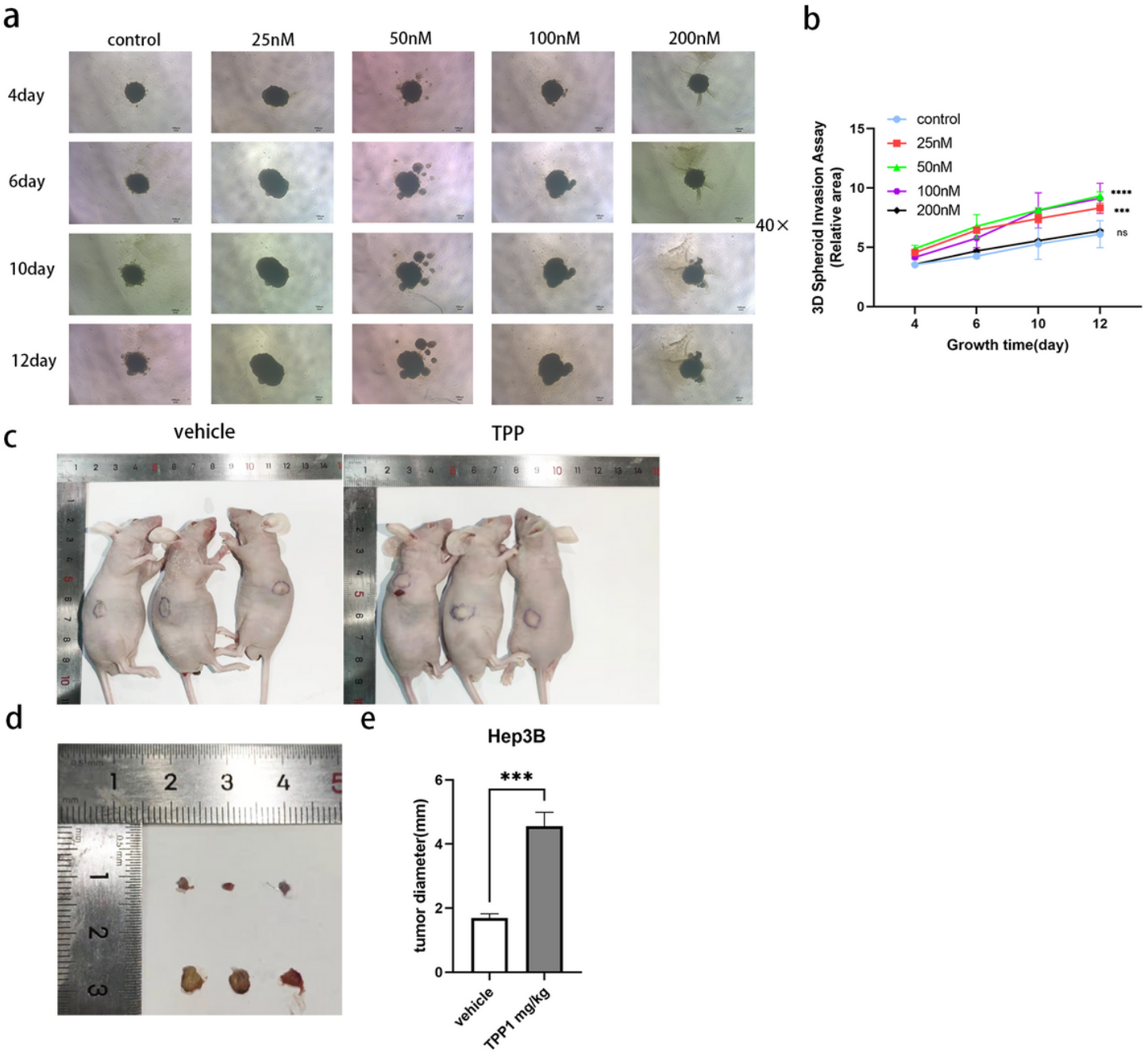

Figure 3

Possible effect of TPP exposure on Hep3B cells migration as determined by the 3D Spheroid Invasion assay and in vivo experiment. (a) Cells were exposed to different concentrations of TPP (0.025μM, 0.05μM, 0.1μM and 0.2μM) and those in the control group were treated with 0.1% DMSO. The cells were cultured for 48h to form spheroids, and then coated by Matrigel. The difference between outward invasion and growth of cell spheroids on day 4, day 6, day 10, and day 12 represent the rate of cell migration. (b) A data graph showing results of 3D Spheroid Invasion assay. The relative area of 0.025μM, 0.05μM, 0.1μM and 0.2μM on day 4 was 4.56±0.25, 4.90±0.27, 4.16±0.15, and 3.56±0.06, respectively, compared to the control group (3.53±0.12). The relative area of 0.025μM, 0.05μM, 0.1μM and 0.2μM on day 6 was 6.44±0.13, 6.77±0.89, 5.77±0.80, and 4.69±0.12 compared to the control group (4.25±0.17). The relative area of 0.025μM, 0.05μM, 0.1μM and 0.2μM on day 10 was 7.42±0.35, 8.13±0.20, 8.11±1.46, and 5.56±0.08, respectively, compared to the control group (5.29±1.17). The relative area of 0.025μM, 0.05μM, 0.1μM and 0.2μM on day 12 was 8.31±0.38, 9.33±0.34, 9.13±1.22, and 6.38±0.09, respectively, compared to control group (6.11±1.04). (c) Total imaged of nude mice. After 14 days, all nude mice were sacrificed, and the tumors were resected to be imaged. (d)The image shows tumor morphology. (e) The graph shows tumors diameter histogram for 14 days of treatment with TPP or vehicle. The error bar represents the mean±SD of at least three independent experiments. (n=3, ****($p<0.0001$), ***($p<0.001$), **($p<0.01$) and *($p<0.05$)).

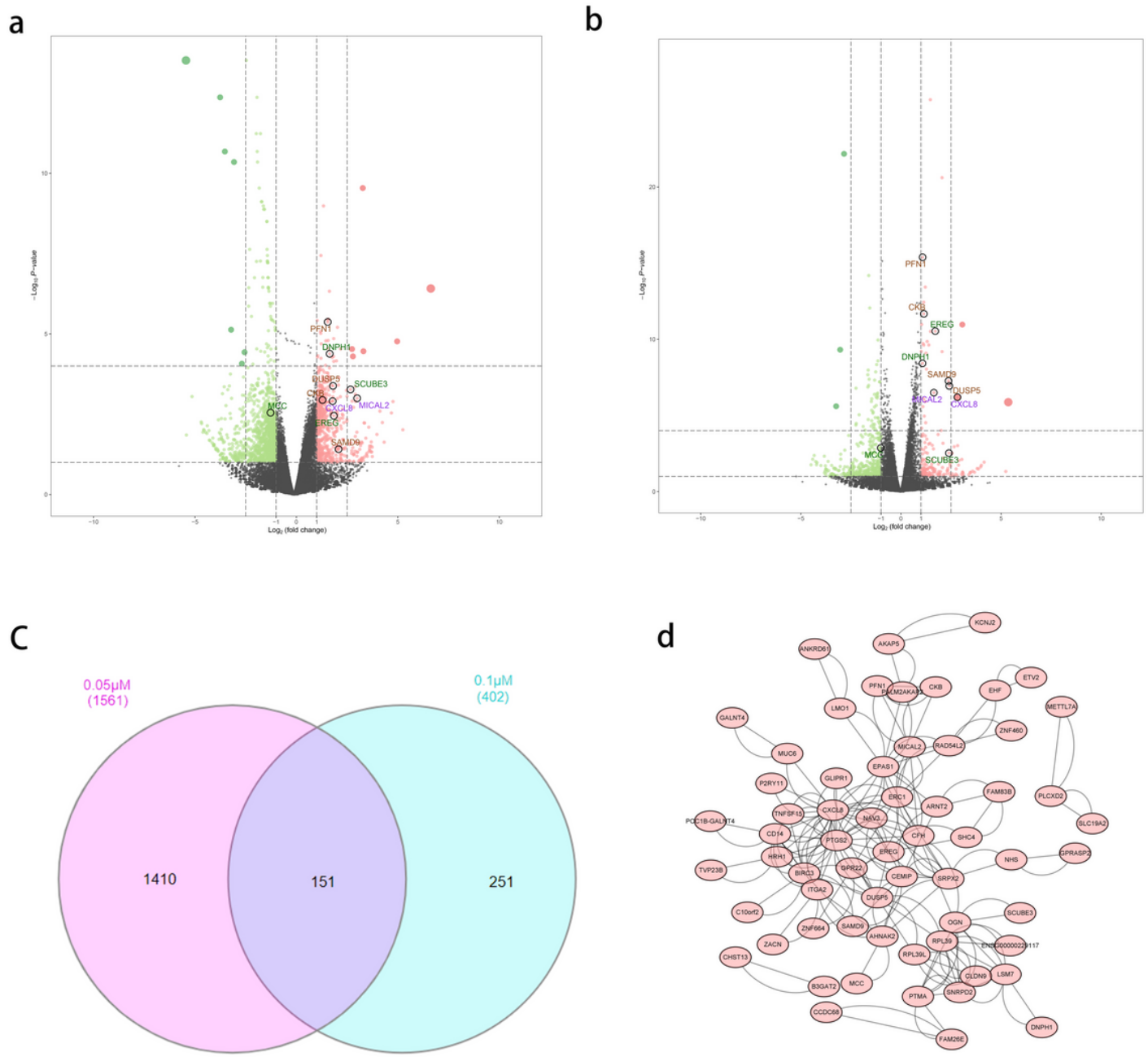

Figure 4

(a) Differential expression genes of RNA-seq data between 0.05μM TPP group and control group; (b) Differential expression genes of RNA-seq data between 0.1μM TPP-treated group and control group; (c) A Venn diagram displaying the co-differentially expressed genes in two differentially expression genes analysis; (d) PPI network of the co-differentially expressed genes.

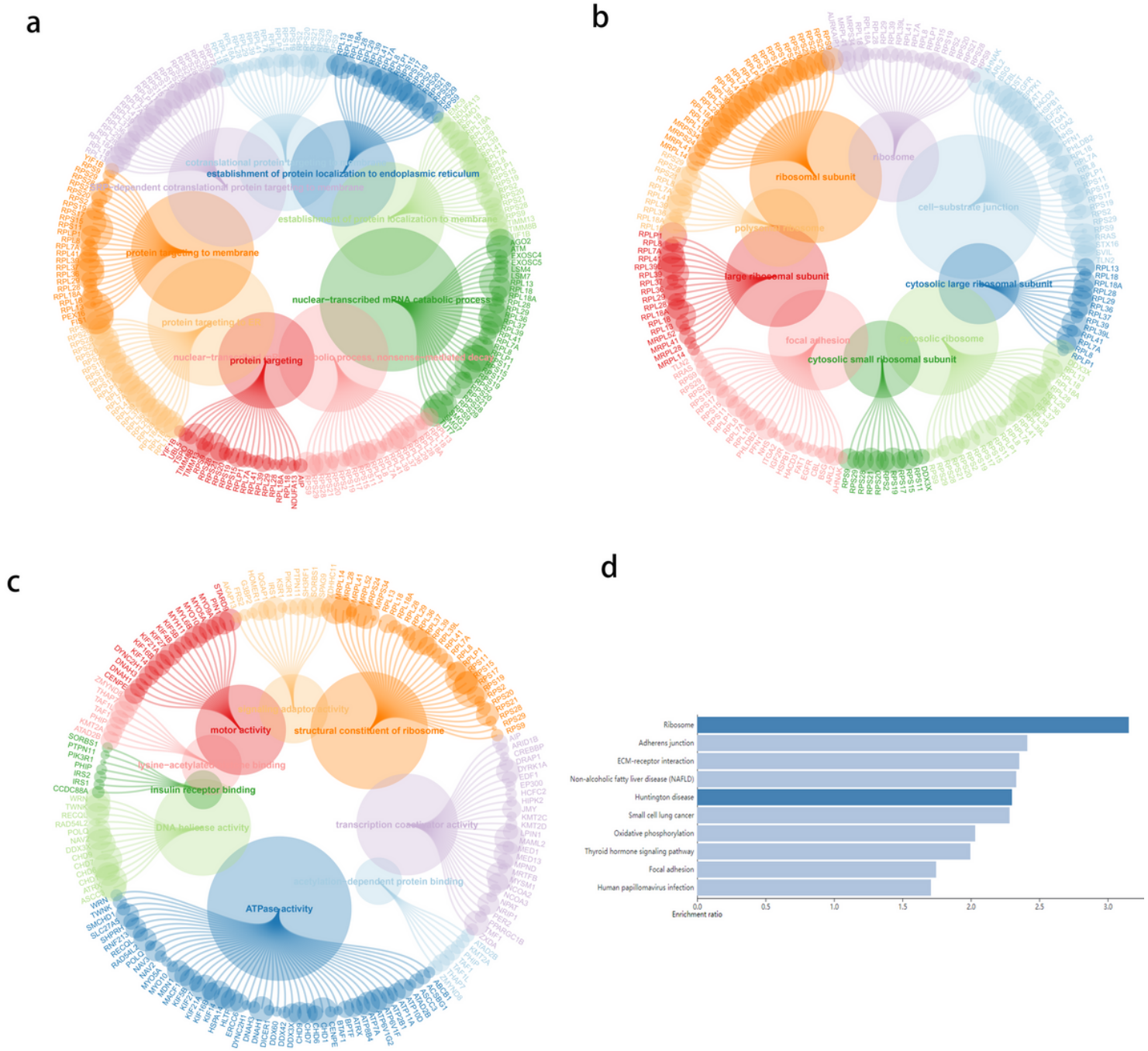

Figure 5

Circle plots showing GO and KEGG enrichment pathways between 0.05μM TPP-treated group and control group. (a) The top terms in GO BP enrichment analysis; (b) The top terms in GO CC enrichment analysis; (c) The top terms in GO MF enrichment analysis; (d) KEGG enrichment pathways.

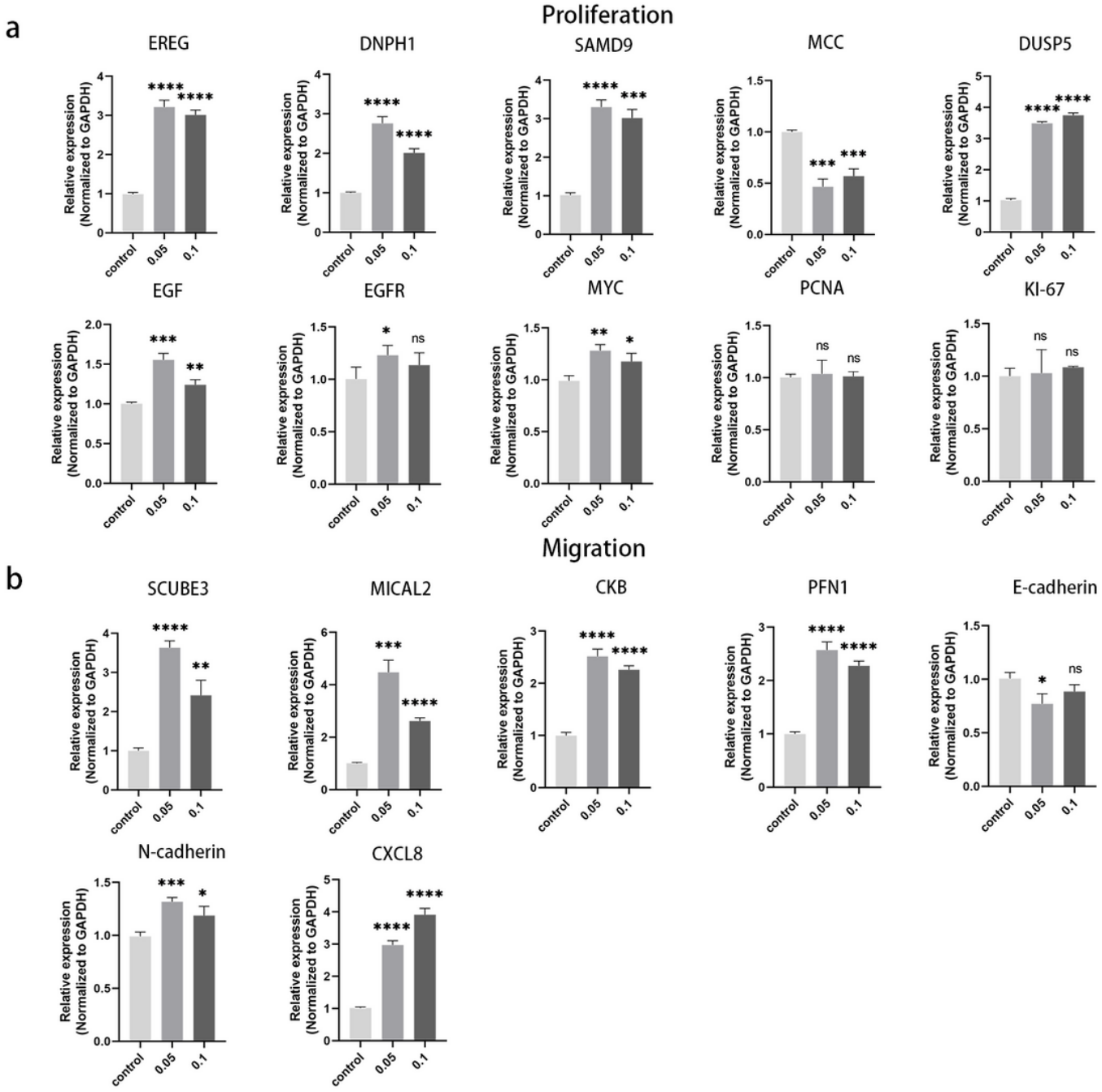

Figure 6

Expression pattern of genes involved in proliferation and migration of Hep3B cells after exposure to 50nM and 100nM TPP for a week. (a) The expression levels of genes associated with the proliferation of Hep3B cells, including *EREG, DNPH1, SAMD9, MCC, DUSP5, EGF, EGFR, MYC, PCNA,* and *KI-67*. (b) The expression levels of genes associated with migration of Hep3B cells, including *CXCL8, MICAL2, SCUBE3, CKB, PFN1*, E-cadherin, and N-cadherin. The error bar represents the mean±SD of at least three repeated experiments. (n=3, ****($p<0.0001$), ***($p<0.001$), **($p<0.01$) and *($p<0.05$)).